

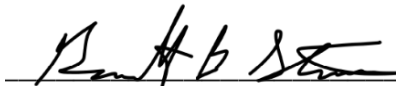
# Identifying Tactile Evidence Accumulation-Based Choice-Related Neural Activity in Mouse PPC-RL

Undergraduate Thesis

by

Ashley Kim

Primary Approver Signature: \_\_\_\_\_



Dr. Garrett Stanley (Stanley Lab)

Co-Mentor: David Weiss, PhD student

College of Engineering

Wallace H. Coulter Department of Biomedical Engineering

*Georgia Institute of Technology*

Secondary Approver Signature: \_\_\_\_\_



Dr. Christian Waiblinger

College of Engineering

Wallace H. Coulter Department of Biomedical Engineering

*Georgia Institute of Technology*



Further, the evidence encoded by the PPC is graded at any given time, increasing proportionally with the average strength of the sensory evidence (Hanks et al., 2015). In a visual evidence accumulation study, authors Raposo et al. (2014) inhibited spiking activity of rat PPC neurons and reliably found impairment to visual discrimination trials. The findings from these studies highlight PPC's causal involvement in decision-making and implications for PPC as more than just a sensory region.

Further, within PPC, the rostrolateral region (RL) has been proposed to be a somatosensory subdivision (Gallero-Salas et al., 2021), and multiple studies have shown RL to receive strong somatosensory inputs (Gilissen et al., 2021; Olcese et al., 2013; Hovde et al., 2019). The exact anatomical definition of RL as a part of PPC has been a topic of debate, and until recently, RL was thought to be a higher order visual area (see Fig. 1 for visual of PPC disparities). Some researchers still consider RL to be a higher order visual area (Sit & Goard, 2020; Wang & Burkhalter, 2007; Weiler et al., 2024), while others believe the region to be part of the PPC (Gilissen et al., 2021; Hovde et al., 2019; Lyamzin & Benucci, 2019; Olcese et al., 2013). These debates leave a critical gap in understanding RL's contribution to tactile evidence accumulation, particularly its role in integrating sensory input into actionable decisions. While RL's direct involvement in tactile evidence accumulation has yet to be concretely defined, its anatomical output connectivity suggests its role in decision-making, as one of the main areas of connectivity is the orbitofrontal cortex, a region highly involved in decision-making activity and reward-processing (Lyamzin & Benucci, 2019; Wallis, 2007). These anatomical studies have been able to identify the neural coordinates for the borders of RL and have shown connectivity between RL and other brain regions that are characteristics of PPC (Gilissen et al. 2021). However, there is yet to be a study that functionally defines RL in terms of its role in processing somatosensory stimuli for decision-making in accumulation of evidence tasks.

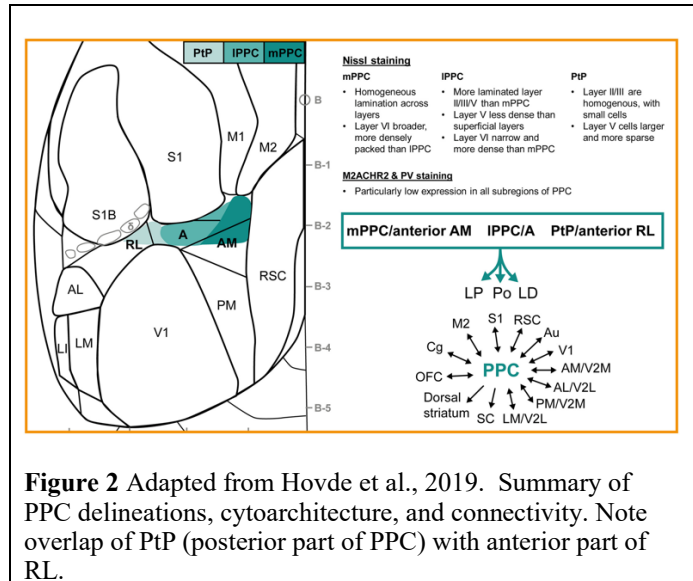
This study aimed to characterize choice-related activity in RL during somatosensory accumulation of evidence to identify it as a posterior parietal region in mice. While the role of PPC in decision-making has been well established across sensory modalities, much less is known about the contribution of its somatosensory subregion, RL. Given its anatomical connectivity and growing evidence for involvement in both tactile and cognitive processing, RL is a compelling candidate for mediating evidence-based decision-making in the somatosensory domain. By identifying choice-selective neurons in RL and characterizing their task-dependent activity, this study sought to functionally identify RL as a part of the mouse PPC. While others (Han & Helmchen, 2024; Gallero-Salas et al., 2021) have found functional evidence for RL as a part of PPC using somatosensory working memory tasks, this study sought to extend these findings to somatosensory evidence accumulation. It is still unclear how RL is involved in cognitive and sensory processing towards behavior. The central question of this study was whether RL neurons encode decision-related signals during tactile evidence accumulation. We hypothesized that RL neurons will exhibit task-specific firing rate modulations that reflect both the animal's choice and the difficulty of the decision, thereby functionally supporting its classification as part of PPC. If RL serves as a true PPC subregion, it should not only receive somatosensory input but also reflect the internal dynamics of decision-making. An evidence accumulation framework provides a powerful lens through which to test this hypothesis, as it enables discrimination

between sensory input, motor response, and intermediate decision states. Neural activity was recorded electrophysiologically with high-density electrodes while animals performed the task. To characterize neural activity, this study analyzed firing rate modulations by comparing firing rates across different trial types and outcome to determine if RL neurons exhibit selectivity for specific task structures. Additionally, we analyzed the temporal dynamics of firing rate changes during the task to assess whether RL neurons present gradual ramping correlated with stimulus presentation. By weaving the findings from anatomical, behavioral, and computational studies, this study sought to identify the neuron-level choice activity of RL to define the region as a part of mouse PPC. We found that RL neurons exhibit task-specific firing rate modulations that reflect both trial difficulty and choice direction, providing functional evidence that RL encodes decision-related signals. These findings support the classification of RL as a subregion of the PPC involved in sensory-to-action transformation during somatosensory decision-making.

## II. Anatomy of Mouse PPC and RL

The anatomy of the mouse PPC with relation to RL has been a point of confusion in terms of its structure and functional relevance in sensory processing. Some researchers believe RL to be a higher order visual area (Sit & Goard, 2020; Wang & Burkhalter, 2007; Weiler et al., 2024), while others believe the region to be part of the PPC (Gilissen et al., 2021; Hovde et al., 2019; Lyamzin & Benucci, 2019; Olcese et al., 2013). Some researchers regard the areas as having multi-functional purposes in both higher order visual and whisker processing (Weiler et al., 2024).

However, while the functionality of RL has been established to be multi-purpose, the anatomical delineations with reference to PPC are still unclear. To establish the borders of PPC based on cellular structure, Hovde et al. (2019) used cytoarchitectural and chemoarchitectural markers/stains and anterograde tracer injections to establish distinct regions of the PPC. The authors focused on three main regions: RL, anteromedial area (AM), and Medio-Medial-Anterior cortex (MMA (see VISRL, VISam, and VISa in Fig. 1). The posterior part of PPC is shown to overlap with the anterior part of RL (Fig. 2). In terms of cortical connectivity, according to Whitlock (2017) and Hovde et al. (2019), a PPC subregion must connect to at least the sensory, motor, retrosplenial, orbitofrontal, and cingulate cortices, in addition to subcortical areas such as the associative thalamic nuclei. These criteria are highlighted in Glissen et al.'s (2021) definition of the afferent connections to RL. The main regions of input to RL include the orbitofrontal cortex, M2, anterior retrosplenial agranular cortex (RSAa), and the



auditory/somatosensory/visual cortices. The regions of output from RL include lateral posterior (LP), lateral dorsal (LD), and posterior (Po) thalamic nuclei. This cortical connectivity provides convincing evidence for RL as a PPC subregion, as it directly meets the criteria for a PPC subregion as proposed by Whitelock (2017) and Hovde et al. (2019).

Despite this progress made in defining RL as a PPC subregion, the classification of RL as both a sensory-processing and decision-making area remains unclear, as there is also convincing literature for RL being a visual area. Research by Sit & Goard (2020) functionally defines RL by highlighting that the processing of visual motion in the mouse cortex is distributed evenly across visual areas, one of those being RL. The authors highlight that RL is a constituent of the dorsal stream by delivering a visual task and analyzing the coherent motion. Additionally, RL appears to be specialized for encoding visual stimuli within reach of the whiskers, suggesting the existence of a visuo-tactile map of near space in RL. Anatomically, Wang & Burkhalter (2007) used triple pathway tracing and receptive field recordings to create a map of V1 and its cortical connections. In this map, the authors identified an orderly representation of the entire visual hemifield (a retinotopic organization) of RL. Connectivity maps in terms of visual field coordinates revealed that projections from V1 were directly mapped to RL. Thus, it becomes clear that there is also convincing evidence for RL as a higher order visual area. There is undeniably conflicting information available in the field regarding both the delineations of PPC and the anatomical categorization of RL as a PPC region or a visual area. However, these conflicting views on RL's role in sensory processing and decision-making directly inform the central research question of this study: whether RL serves as a sensory-processing area or a decision-related region within the PPC. The anatomical and functional studies reviewed here highlight the need for further exploration of RL's role in cognitive and sensory processing towards behavior.

### **III. Evidence Accumulation and Decision Modeling**

PPC has been established to play a role in decision-making in rodents (Goard et al., 2016; Harvey et al., 2012, Raposo et al., 2014). Further, PPC has been causally suggested to be necessary for decision-making with visual stimulus presentation (Goard et al., 2016; Harvey et al., 2012; Hwang et al., 2017; Licata et al., 2017). In a visual go/no-go lick-based discrimination task, authors Pho et al. (2018) sought to identify PPC's specific role in sensory processing/sensorimotor transformation. They found that PPC activity is strongly task-dependent, with the majority of PPC neurons showing no significant responses when passively viewing stimuli. Additionally, the activity of PPC neurons is strongly biased toward the target stimulus, indicating that there are cognitive variables correlated with the learned association between the target stimulus and the reward. To test whether PPC neurons were more sensitive to stimulus or choice, the authors re-trained animals on the reverse sensorimotor contingency. They found that PPC neurons became selective to the new target stimulus, V1 while remained preferential to the original stimulus. While the stereotaxic coordinates used in Pho et al. (2018) correlate to region AM (anteromedial area), this study still provides important implications for the current project and the predictions for our tactile discrimination task results. Specifically, in RL, studies have demonstrated its involvement in the integration of multisensory inputs. In a

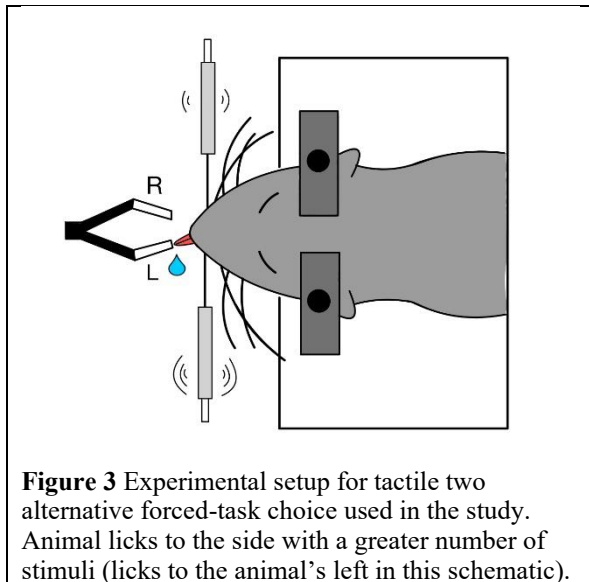
multisensory modality task (tactile and auditory), authors Han & Helmchen (2024) were able to identify PPC-RL as more highly involved in texture and reward processing, compared to PPC-A (anterior region) and S1 which were only tuned to the texture processing. This suggests RL's role in decision-reward circuits and further establishes it as more than just a sensory region, highlighting RL's involvement in making perceptual decisions.

In terms of modeling the accumulation of evidence in animals, Brunton et al. (2013) developed a framework in which rats could reliably accumulate pulsatile sensory evidence over time and make accurate decisions. Their task design, which delivered evidence in randomized pulses, allowed animals to gradually integrate information and minimized the influence of non-perceptual noise. This model provided a strong foundation for examining how evidence accumulation unfolds across trials. However, while evidence accumulation is critical for understanding decision-making, Gupta et al. (2024) highlight an important nuance: trial history can significantly bias the accumulation process. They show that what may appear as lapses, (random, evidence-independent errors) are often better explained by deterministic history biases embedded in the accumulation process. Specifically, they propose a model where the initial state of the accumulator is updated based on prior outcomes, which can shift psychometric thresholds and affect lapse rates. This finding suggests that animals may not treat each trial in isolation but instead carry forward prior expectations, especially in tasks with subtle or ambiguous evidence. Incorporating this insight, our task design allows us to study decision-making within a framework that acknowledges both the sensory-driven accumulation of evidence and the role of internal trial history biases. This is especially relevant for interpreting RL neural activity, as neurons may encode not just the current stimulus but also belief states shaped by prior experience.

## **IV. Methods**

### 1.1 Subjects

All experiments use 10–26-week-old mice of type C57BL/6 or genotypic negative NR133xAi32. The sample size of this study was 4 (2 female mice, 2 male mouse). All experimental animals are placed on a reverse light cycle to promote wakefulness and task engagement during the daytime. Animals have free, unrestricted access to food but are water-restricted to induce a reward-based motivation. This approach has been extensively validated in similar behavioral paradigms to reliably enhance task performance while maintaining animal health. The water schedule used is as follows: 2-4 hours per day during task training (2 hours/session), typically 5-7 days a week. On days in which the animals were not trained, 1.5 mL of water were given to the animal. Training sessions were held 1-2 times a day. Animals are weighed before and after each session to track water consumption, and their weights were closely monitored in order to ensure proper health. All animal procedures and experiments were performed in accordance with protocols approved by the Georgia Institute of Technology Animal Care and Use Committee (protocol A100223). <sup>[OB]</sup>



## 1.2 Behavioral Task

The two-alternative forced-choice task was specifically designed to test the ability of RL neurons to encode sensory evidence during decision-making. For this task, mice are trained in a custom-made training setup consisting of a head-fixing platform, a right/left lick detector, and an analog galvanometer with an attachment that allows for single whisker threading (Figure 3). The two-alternative forced choice entails discriminating between the number of stimuli to the right/left and licking the corresponding side of the lick detector's spout. Stimuli come from two simultaneous streams of random, discrete stimuli to the left and right whiskers. The animals were considered to have successfully learned the task once they achieved at least 75% accuracy. This performance threshold had to be met while the animal was engaged in the most difficult version of the task, defined by a stimulus distribution with a standard deviation of 10 and a single Gaussian distribution for stimulus delivery. These parameters minimized the difference in the number of left and right whisker stimulations, increasing the reliance on sensory evidence for decision-making. This ensured minimal differences in the number of left and right whisker stimulations, emphasizing decision-making based on the tactile stimuli.

To reduce noise from impulsive licking and to isolate decision-related neural activity, specific behavioral constraints were implemented in the latter two animal recordings. Animals were required to wait for a 2-second pretrial interval; any licking during this interval aborted the trial. Similarly, licking during stimulus delivery ended the trial prematurely. Animals had to wait a minimum of 250 ms after the stimulus offset before making their choice. A failure to lick within the 3-second response window after stimulus delivery was classified as a "miss" trial.

During the task, white noise and red lights in the room were used to encourage focus on the task without distractions. Additionally, to aid with preventing impulsive licking (which would cause many aborted trials), a stimulus cue light was used to indicate when the animals should not lick. Total water intake was measured using weight, comparing initial weight in grams to final weight and subtracting the difference to measure milliliters of water consumed. We regularly monitored animals' engagement and bias levels, making adjustments to the

difficulty and reward amount as needed. By implementing this adaptive training model, we sustained motivation throughout the data collection period while maintaining the overall task structure.

### 1.3 Analysis

Data collection was performed electrophysiologically. Using multiple-electrode recordings, we were able to identify the simultaneous spiking activity of many neurons at once. This technique allows us to understand how groups of neurons in RL act together to define its functions (Brown et al., 2004). In order to ensure precise placement of the probe within region RL, intrinsic optical imaging (IOI) was used to identify the region in relation to the barrel cortex (Berwick et al., 2002). In each session, there were many trials (100-150), and there were slight differences in behavior and neural activity. This combined with noise can lead to considerable variability in spike timing (Kass et al., 2018). Thus, implementing spike sorting thresholds and criteria across an entire session (100-150 trials) allowed us to identify spikes and mitigate this inherent variability. Through this process of spike sorting, single units are identified for each session.

To analyze the resulting spike trains, we employed statistical comparisons between defined behavioral conditions to identify neurons that significantly modulated their activity based on task-relevant variables. Given the trial-to-trial variability and non-normal distribution often seen in neural data, non-parametric tests (Wilcoxon rank-sum, Kruskal-Wallis) were used in initial comparisons of firing rates between conditions. For paired within-neuron analyses, paired t-tests were also used where appropriate, particularly when comparing firing rates across matched stimulus windows. These tests allow us to assess whether observed differences in neural activity reflect genuine task-driven modulation rather than random fluctuations.

## **V. Results**

To begin characterizing choice-related neural activity in RL, we first compared firing rates during trials in which a behavioral response was made (Answered) versus trials in which no response occurred (Miss). This comparison provides a broad initial look at task engagement and potential decision-related modulation. Although Answered trials include both correct and incorrect responses, they reflect the presence of an action, distinguishing them from Miss trials, which primarily reflect stimulus processing in the absence of a behavioral choice. While these findings indicate a task-related modulation in RL, a significant difference between conditions does not necessarily imply choice selectivity. For example, as shown in Figure 1c, Neuron 27 displays higher firing rate activity during Miss trials. Since both trial types include sensory information, this activity could reflect stronger sensory response, a disengagement from motor planning, or even internal state differences such as attention or arousal. Further, the absence of licking in Miss trials does not reveal the animal's internal decision: the mouse may have perceived the stimulus but chosen to withhold a response, may have attempted to respond but failed to contact the lick spout, or may not have attended to the stimulus at all. Because of this ambiguity, we interpret these differences as broadly task-modulated, but not necessarily as evidence for decision or choice encoding.

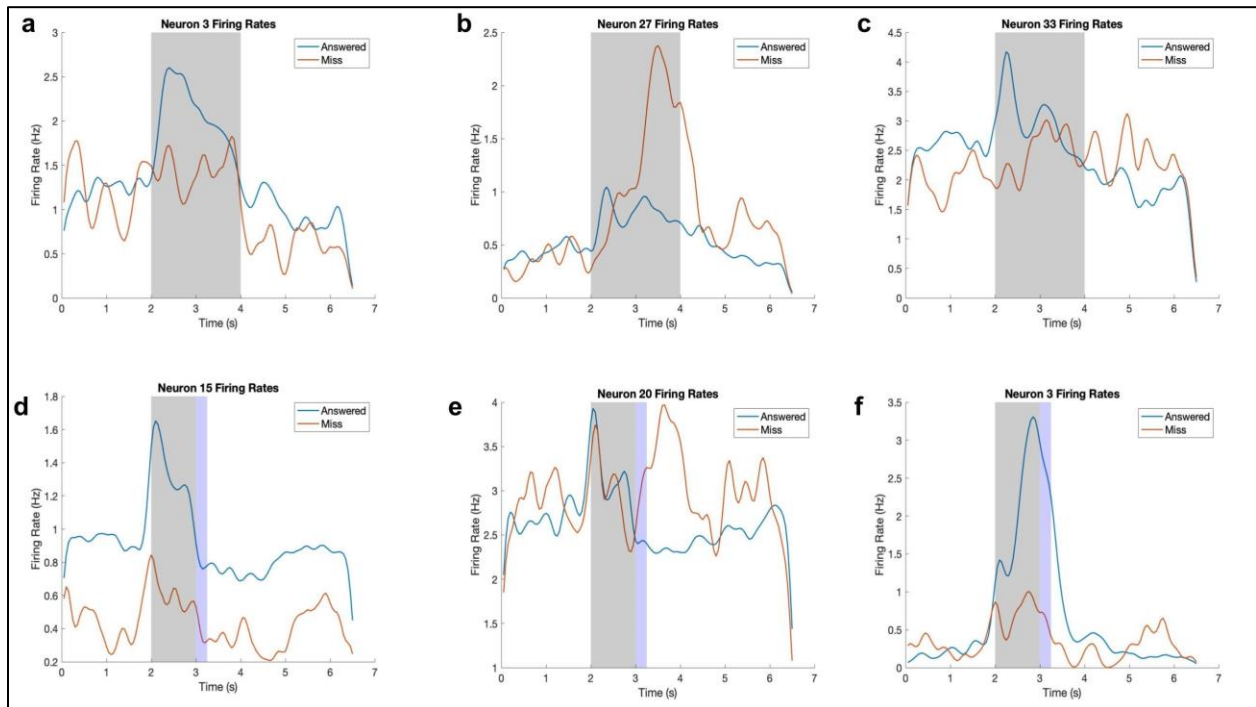


**Figure 1.** 1a–1c represent the single unit firing rates during Answered (blue) and Miss (red) trials in mice that were not subjected to a delay period constraint, with the “stimulus on” window (2–4 s) shaded in gray. 1d–1f show comparable data from animals with a 250 ms enforced delay denoted by a light blue shaded region and “stimulus on” window (2–3 s). All neurons were found to exhibit statistically significant differences between Answered and Miss trials during the stimulus period (Kruskal-Wallis test,  $p < 0.05$ )

One method for distinguishing between sensation-responsive and choice-responsive neurons involves aligning neural activity to the moment of the animal’s first lick, indicating its decision (Fig. 2). This alignment serves as a behavioral reference point that is independent of task time and allows for assessing neural responses in relation to the decision-making action itself. We compared single unit firing rates before and after the decision report (lick) to assess the dynamic neural representation of the execution of choice. Notably, all neurons that were significantly modulated across this window displayed a decrease in firing rate following the lick. This highlights the dynamic neural modulation associated with the execution of a choice. As seen in Figure 2b, the concentration of spikes noticeably builds up in the second preceding the lick at  $x = 0$  and then becomes sparser. This decrease has two possible explanations. The first is that there is post-lick suppression as a result of the execution of choice. The second is that the neurons ramp in response to decision formation and return to baseline post-lick ( $x = 0$ ). Both explanations support the idea that these neurons are engaged in choice-related processing rather than merely responding to sensory input. If the neurons were solely driven by external sensory stimuli, their activity would be expected to follow the timing of stimulus presentation uniformly across trials, rather than aligning with the behavioral output. Instead, the fact that neural activity consistently peaks just before the lick suggests these neurons are tracking internally generated

decision signals or preparing motor output. The sharp decline in firing post-lick further indicates that their activity is temporally bound to the act of decision, supporting a role in encoding decision execution rather than passive stimulus reception. Among the neurons that were previously found to differ significantly between Answered and Miss trials (Figure 1), approximately half (48.2%) also showed significant modulation around the lick, further refining the population of neurons likely involved in decision making.

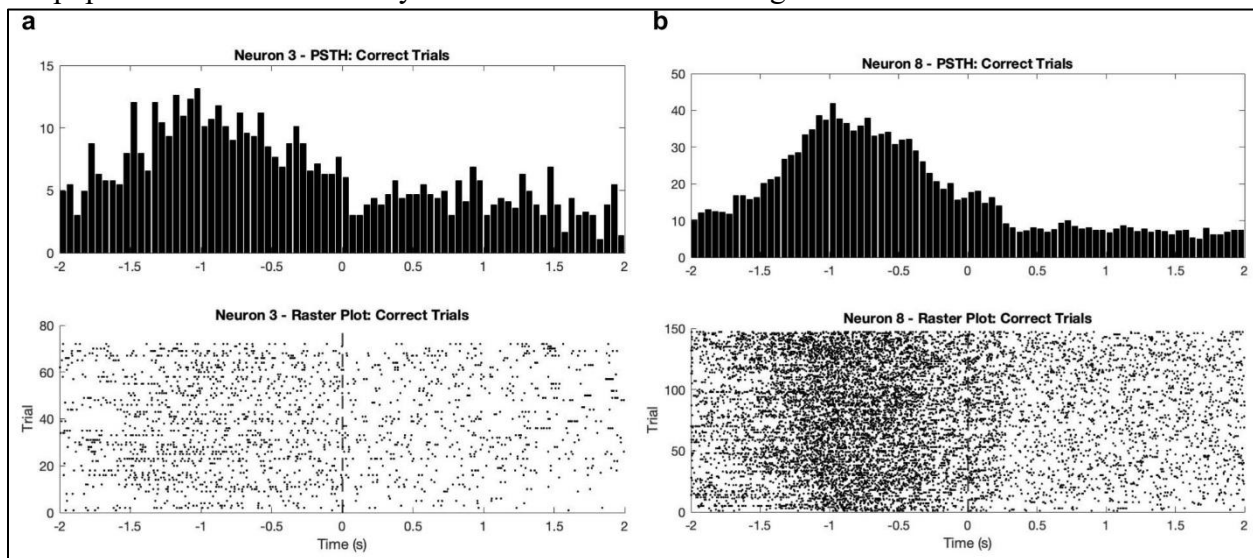


**Figure 2** Neural responses aligned to the first lick for neurons significantly modulated after the lick. Each panel displays a peri-stimulus time histogram (PSTH, top) and corresponding raster plot (bottom) for a single neuron, aligned to the animal's first lick ( $x = 0$ , dashed vertical line). Each small dot represents a spike in the trial. Neurons shown exhibited significant changes in firing rate between the 0.5 sec before versus 0.5 sec after the lick (Wilcoxon signed-rank test,  $p < 0.05$ ).

We can further analyze choice behavior by examining the activity of neurons during Left- and Right-choice trials (Fig. 3). At the single-neuron level, differences were observed in firing rates between Left, Right, and Miss trials, suggesting that individual neurons exhibit preferences for specific choices. To quantify choice selectivity, we compared the average firing rates during the stimulus period in Left and Right trials relative to the average pre-stimulus firing rate across all trials (Fig. 3a). Neurons with larger vertical separation between the two points are more selective, showing a stronger differential response to choice direction. Neurons with larger deviations from the baseline ( $y = 0$ ) indicate stronger modulation from baseline activity. Interestingly, not all neurons demonstrated symmetric responses. Some responded more strongly to one choice direction over the other, while others showed increased firing relative to baseline without differentiating between Left and Right choices. For instance, Neuron 11 in Figure 3a exhibits significant deviation from baseline but no significant difference between Left and Right firing rates. These neurons may reflect general task engagement or stimulus responsiveness rather than encoding of choice.

Choice-selective neurons were defined as those with statistically significant differences both between Left and Right firing rates and relative to baseline (Wilcoxon rank-sum test,  $p < 0.05$ ). Using this criterion, we identified Left- and Right-choice neurons and then calculated the

directionality of each neuron by subtracting average Left trial activity from Right trial activity during the stimulus period (2–4 seconds for no delay animals, 2-3 seconds for delay animals). Figures 3b and 3c show the normalized firing rates of all identified Left- and Right-choice neurons, respectively, pooled across the three sessions with the highest percent correct (one per animal). We identified 20 total Left-choice neurons and 19 total Right-choice neurons out of 68 total neurons across the three sessions. Of this population, there were some differences in the number of identified Left and Right neurons per session (Table 1). While all sessions had Left- and Right-choice neurons, Left-choice neurons were more prevalent in session 1 and decreased across sessions, while Right-choice neurons were more prevalent in sessions 2 and 3. Furthermore, 50.0% of all identified Left-choice neurons came from session 1, whereas the largest proportion of Left-choice neurons (42.1%) came from session 3. This pattern may reflect differences in task strategy across animals, where some mice may have relied more heavily on one decision pathway or circuit than others during training. Additionally, variability in session dynamics, such as differences in attention, arousal, or engagement with the task, could have influenced the recruitment of specific neural populations.

While choice-selective neurons were identified based on higher average firing rates during their preferred choice trials, the population-level dynamics in Figures 3b and 3c offer additional insight into their temporal dynamics. Right-choice neurons (Fig. 3b) show a sharp increase in firing during Right trials following stimulus onset, peaking around 2.5 seconds and then sharply declining after. In contrast, the firing rate during Left trials remains lower and shows more of a gradual decline after stimulus onset. Left-choice neurons (Fig. 3c), however, exhibit a more sustained elevation in firing during Left trials, with broader and more prolonged activity. This is evident from the wider separation between trial conditions that persists beyond the peak. Interestingly, while the average peak firing rate is similar across both Right and Left trials, the post-peak decay appears faster in Right-choice neurons than in Left-choice neurons, suggesting that Left-choice neurons may be maintained longer through the decision process. These temporal differences hint at potential asymmetries in how RL neurons support decision-making across trial types. Right-choice neurons may be more tightly locked to early decision signals, while Left-choice neurons may encode information over a broader window, possibly contributing to sustained accumulation or working memory processes.

To investigate whether particular cell types are preferentially involved in choice selectivity, we examined the spike waveform characteristics of all choice-selective neurons to classify them as regular spiking (RS) or fast spiking (FS). RS neurons are typically excitatory cells, while FS neurons are generally associated with inhibitory interneurons (Tremblay et al., 2016). Of the population of choice-selective neurons with waveform analysis completed, (11 Left-choice, 8 Right-choice), the vast majority were classified as FS (78.9%), with only 4 total neurons classified as RS (7.4%). Specifically, 9 out of 11 Left-choice neurons and 6 out of 8 Right-choice neurons were RS. Both Left- and Right-choice neurons had two FS neurons each. This predominance of FS neurons among the choice-selective population suggests that inhibitory interneurons may play a more prominent role in decision-related processing within RL than previously assumed. This could reflect a circuit-level mechanism in which inhibition helps shape

or gate choice representations, potentially by refining temporal precision or suppressing competing motor plans.

<b>Session #</b>	<b>% Left-choice neuron in session</b>	<b>% Right-choice neuron in session</b>	<b>% of all Left-choice neurons</b>	<b>% of all Right-choice neurons</b>
<b>1</b>	43.5% (10/23)	17.4% (4/23)	50.0% (10/20)	21.1% (4/19)
<b>2</b>	27.3% (6/22)	31.8% (7/22)	30.0% (6/20)	36.8% (7/19)
<b>3</b>	17.3% (4/23)	34.8% (8/23)	20.0% (4/20)	42.1 (8/19)

**Table 1.** Distribution of Left- and Right-choice neurons across sessions. This table summarizes the proportions of neurons classified as Left-choice or Right-choice within each recording session. The first two columns indicate the percentage and count of choice-selective neurons relative to the total number of neurons recorded in each session (# of choice neurons/total neurons in session). The final two columns show the distribution of choice neurons across sessions as a percentage of the total number of Left-choice (n = 27) or Right-choice neurons (n = 13) identified across all sessions.

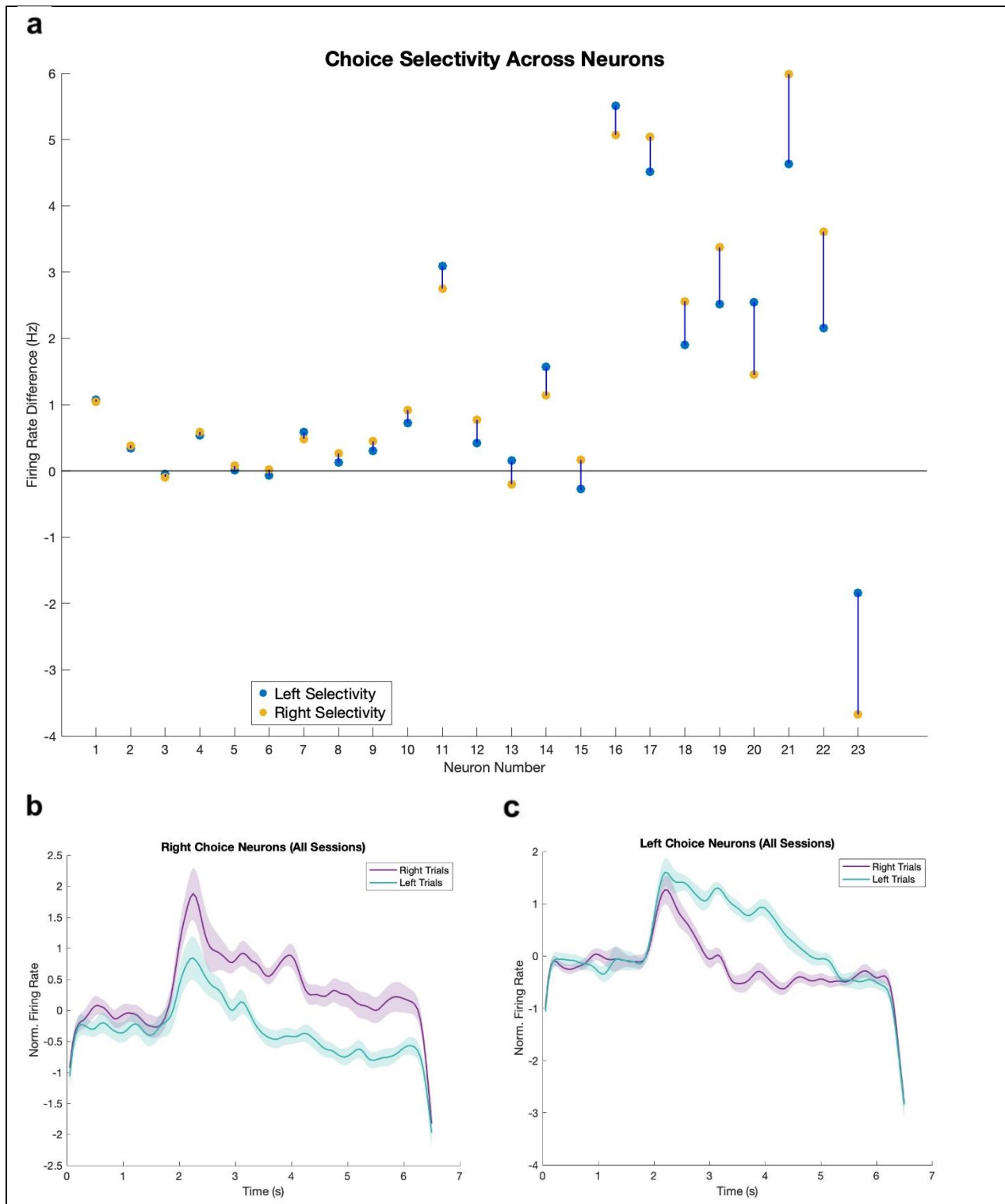


**Figure 3** a) Firing rate modulation by neuron, with Left-choice activity in blue and Right-choice activity in yellow. Each line connects the Left and Right values for a given neuron, sorted by the absolute difference in firing rate between the two conditions (their selectivity). b) Firing rate for Left and Right trials for Left-choice neurons and Right-choice neurons from all sessions. Error bands reflect the standard error of the mean across neurons (Wilcoxon signed-rank test,  $p < 0.05$ ; paired t-test,  $\alpha = 0.05$ ).

We further analyzed patterns of choice behavior by examining firing rate activity across different levels of trial difficulty (Fig. 4). Trials were categorized based on the whisker deflection difference between the left and right whiskers. "Easy" trials had a large deflection difference of 20–30 (e.g., 3 left vs. 23 right deflections), and "Hard" trials had a smaller difference of 0–9. This was then split up further into Left and Right trials. To investigate whether task difficulty influenced neural responses, we computed the percentage of choice-selective neurons (Kruskal-Wallis,  $p < 0.05$ ) in each session. Interestingly, the two animals that performed the task without a delay period had a higher proportion of neurons with significant differences between Easy and Hard trials (47.8% of Right-choice neurons and 43.4% of Left-choice neurons) compared to the animal with a delay period (17.3% Right, 30.4% Left). This suggests that the presence of a delay may reduce the strength or clarity of task-related neural modulation, potentially by separating stimulus processing from motor planning.

When the Hard category was subdivided further, additional patterns emerged. Figure 4d shows firing rates split into "Harder" (difference of 4–8) and "Hardest" (difference of 0–3) trials. A subset of neurons showed selectivity between Harder and Hardest trials, even when no significant difference was observed between Easy and Hard trials. For example, among neurons tested on Harder versus Hardest Right trials, 4 of 15 (26.7%) showed significance only at this finer difficulty resolution. Similarly, in Left trials, 3 of 13 significant neurons (23.1%) were newly significant in the Harder vs. Hardest comparison. Conversely, some neurons that showed significant differences in the broader Easy vs. Hard comparison did not retain significance when comparing Harder vs. Hardest trials. For Right-choice neurons, 3 of 14 previously significant neurons (21.4%) lost significance in the finer-grained comparison; for Left-choice neurons, this was 3 of 8 (37.5%). These findings suggest that some neurons may be more finely tuned to subtle differences in trial difficulty, while others respond to larger distinctions, such as between clearly easy and clearly difficult trials.

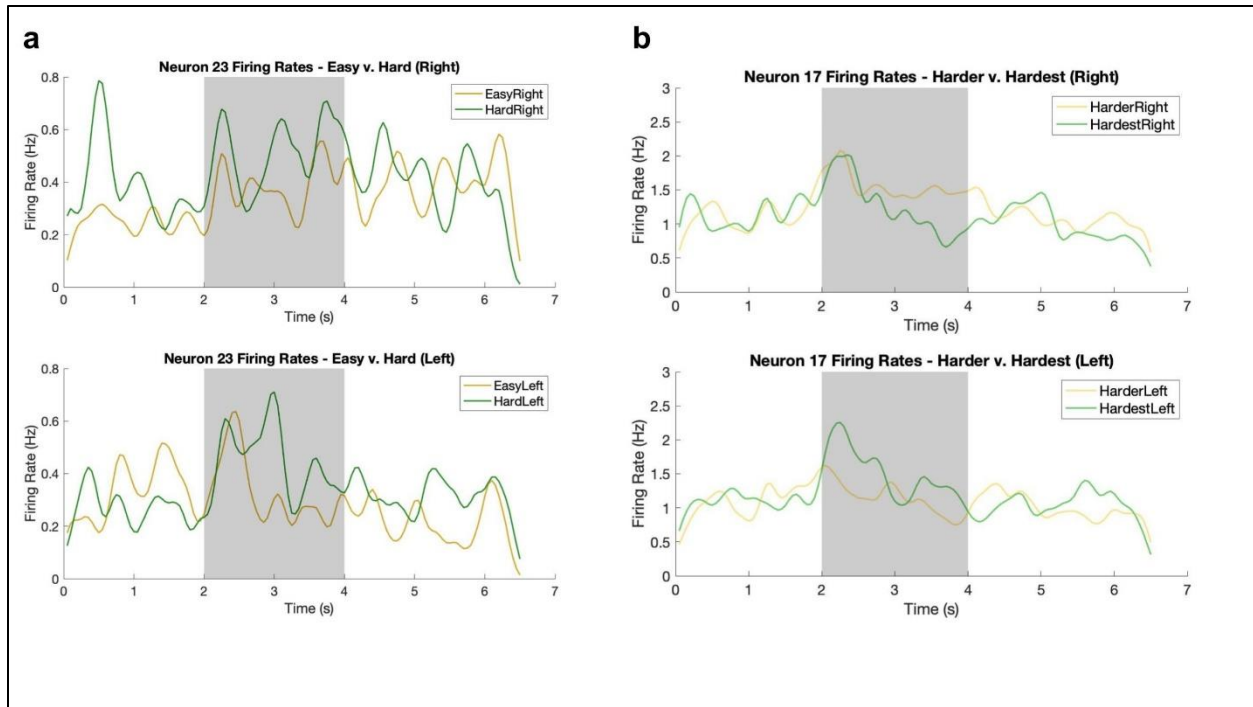


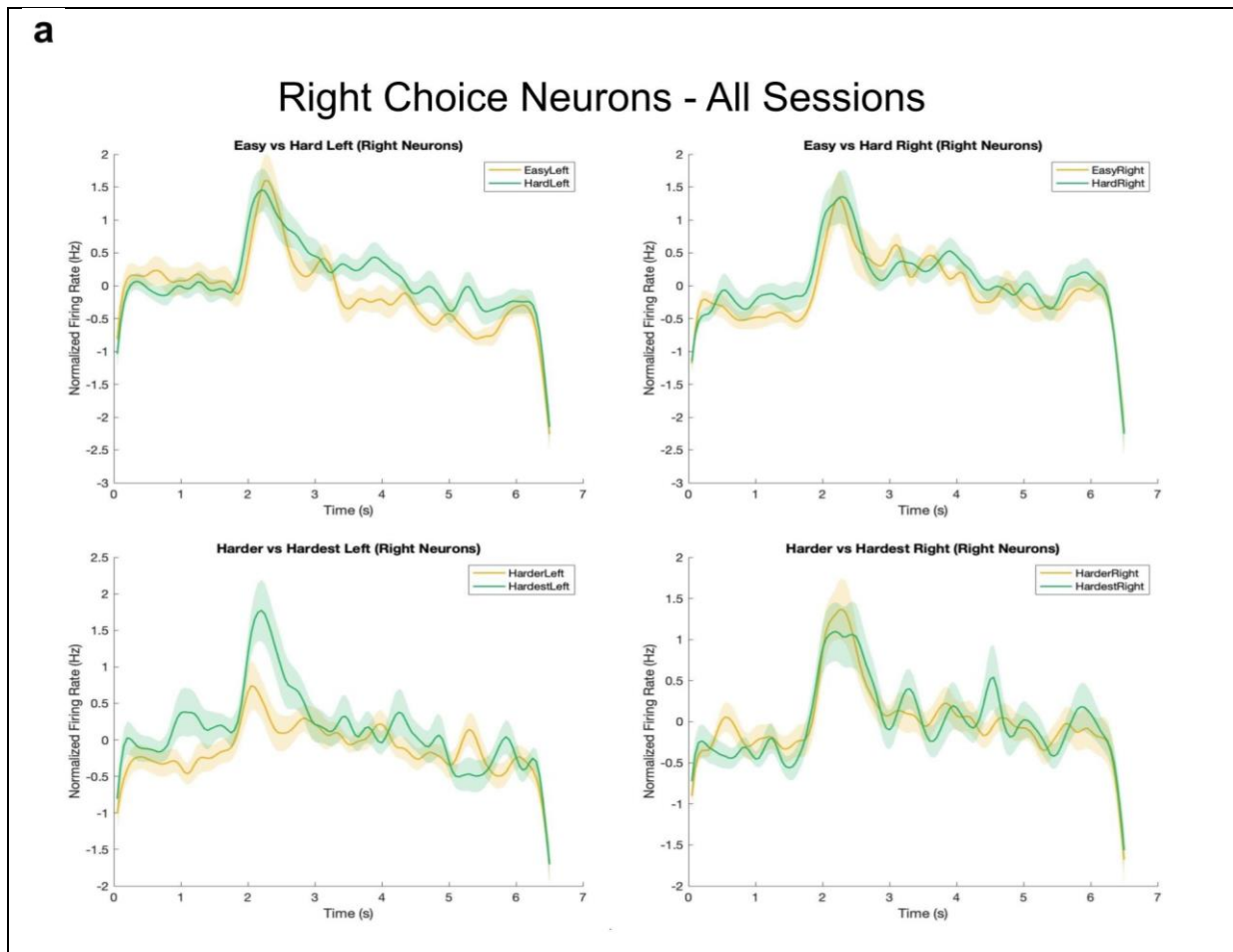
**Figure 4** Firing rate responses of two single RL neurons during Easy/Hard and Harder/Hardest trials, separated by choice direction. Each panel displays smoothed average firing rates during Right (top) and Left (bottom) choice trials. a) Trials are grouped by difficulty: Easy (gold) and Hard (green) and b) Harder (yellow) and Lime (Hardest). Neuron 17 displays significant differences between Easy/Hard left *and* right trials. Neuron 23 displays significant differences between Harder/Hardest left *and* right trials. The shaded region (2–4 s) represents the stimulus presentation window (Wilcoxon signed-rank test,  $p < 0.05$ ).

To further characterize task-relevant subpopulations of RL neurons, we compared firing rates across different levels of trial difficulty within the previously identified left-choice and Right-choice neurons. This analysis included eight conditions in total: comparisons between Easy and Hard trials and Harder and Hardest trials, each split by trial side (Left or Right) and neuron group (Left-choice or Right-choice).

Among Right-choice neurons (Fig. 5a), 72.5% of the population showed significant differences between Easy and Hard trials. These neurons also had some mixed preferences between difficulty levels: 14 out of 16 significantly modulated neurons had higher firing rates during Hard-Left trials, but only 6 out of 17 significant neurons preferred Hard-Right over Easy-Right trials. This suggests that Right-choice neurons may be particularly sensitive to increases in task difficulty on the contralateral side (Left trials) but show more varied responses to difficulty changes on the ipsilateral side. In the Harder versus Hardest comparison, Left-choice neurons showed a similar trend to Right-choice neurons, with increased firing during the Hardest trials (specifically, 88.2% preferred Hardest-Left trials and 63.6% preferred Hardest-Right trials).

For Right-choice neurons (Fig. 5b), 77.5% showed significant differences between Easy and Hard trials on at least one trial side (paired t-test,  $\alpha = 0.05$ ). However, the direction of modulation varied across trial types. During Left trials, 12 of the 16 significant neurons showed

higher firing rates during Easy-Left trials than Hard-Left trials. In Right-side trials, responses were more mixed: 8 neurons preferred Easy trials, while 7 showed higher firing during Hard trials. This indicates that some neurons may scale their responses with stimulus difficulty or ambiguity, while others may be more responsive when choice direction is more clearly defined. In the Harder vs. Hardest comparisons, 52.5% of Left-choice neurons were significantly modulated. Notably, the majority of neurons responded more intensely to the Hardest condition for both Right (63.6%) and Left trials (70.0%). Interestingly, for both neuron groups, a higher percentage of significant neurons emerged when trial difficulty was ipsilateral to the neuron's choice selectivity (e.g. Left trials for Left-choice neurons).



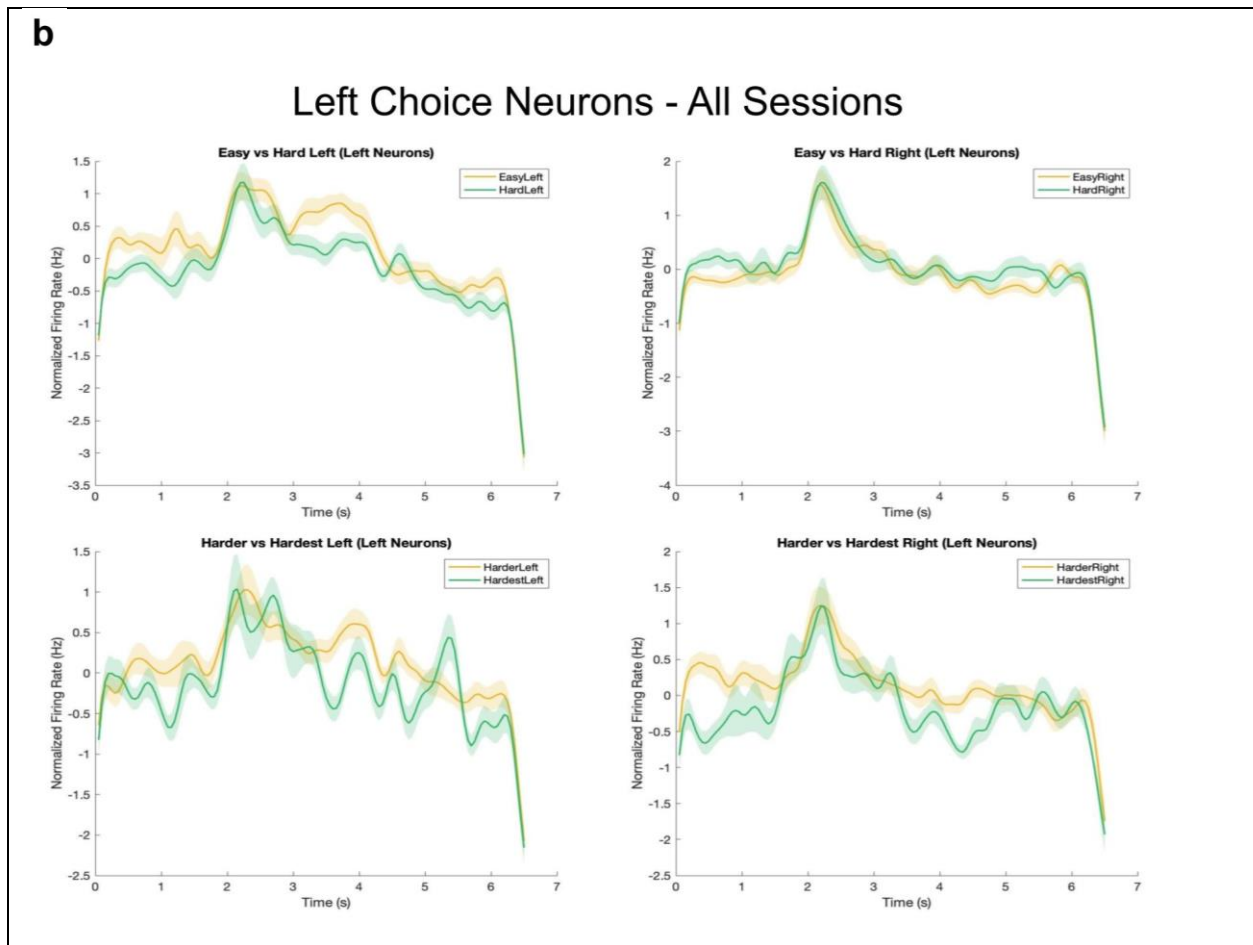


**Figure 5** a) Average normalized firing rate responses of Left- and b) Right choice-selective neurons across Easy, Hard, Harder, and Hardest trials. Each panel displays firing rates across all identified left choice neurons during specific trial conditions. Trials are grouped by difficulty level for Left (left panel) and Right (right panel) choice trials: Easy (yellow) vs. Hard (green). Bottom: Trials are grouped into Harder (yellow) vs. Hardest (green) for Left- and Right-choice trials. Error bands reflect the standard error of the mean across neurons (Wilcoxon signed-rank test,  $p < 0.05$ ).

## VI. Discussion

This study aimed to functionally characterize the role of the rostralateral (RL) area in the mouse cortex during a somatosensory decision-making task. While anatomical studies have suggested RL may serve as a subregion of the posterior parietal cortex (PPC), its functional contribution to evidence accumulation and decision-making has remained ambiguous. By analyzing choice-related neural activity in RL, we provide new insights into how this region may support the transformation of sensory input into behaviorally relevant choices. Our findings demonstrate that RL neurons show distinct firing rate modulations based on task engagement and decision outcomes. Neurons were significantly more active during trials in which the animal made a behavioral response ("Answered") compared to when it did not ("Miss"), indicating task-

related modulation. However, this modulation alone was not sufficient to conclude that RL neurons encode choice-specific signals. To address this, we aligned neural activity to the animal's first lick, a behavioral marker of decision execution, and found significant changes in firing rate surrounding the choice event. Importantly, many of these neurons showed suppression following the lick, suggesting they may play a role in preparatory or decision-related activity rather than purely sensory processing. To further refine the population of neurons involved in decision-making, we analyzed firing rate activity across trials grouped by choice direction. Some neurons exhibited significant and consistent differences in firing between Left and Right trials, beyond changes in baseline activity. Interestingly, these choice-selective neurons often showed asymmetric responses, with a preference for one direction and minimal modulation for the other. This supports the view that RL encodes choice not in a binary manner, but through a population code in which different neurons reflect varying degrees of selectivity. These findings are consistent with previous work demonstrating choice-related activity in the PPC of rodents (Pho et al., 2018; Raposo et al., 2014) and extend this work to the somatosensory domain. Our findings also contribute to ongoing debates about RL's classification by functionally linking it to decision variables, complementing anatomical evidence suggesting RL belongs to the PPC (Gilissen et al., 2021; Hovde et al., 2019).

At the population level, the temporal dynamics of neurons further clarify their roles in decision formation. Right-choice neurons showed a sharp increase in firing rate during Right trials following stimulus onset, peaking early and decaying quickly. Left-choice neurons, in contrast, exhibited more sustained firing across the stimulus period, suggesting possible involvement in holding decision-related information over time. These differences hint at functional asymmetries in RL activity, with potential implications for how evidence is accumulated and maintained. We also investigated how RL neurons respond to variations in trial difficulty. When trials were grouped as Easy or Hard based on whisker deflection differences, a majority of both Left- and Right-choice neurons showed significant modulation, although the direction of this modulation varied. Some neurons fired more during Hard trials, potentially reflecting increased cognitive demand or sensory integration under ambiguous conditions. Others preferred Easy trials, which may reflect stronger sensory signals or greater confidence in decision-making. When the Hard trials were further split into "Harder" and "Hardest," we identified neurons that responded selectively to these finer levels of difficulty. Some neurons that did not show significance in the Easy versus Hard comparison were tuned to these subtle differences, while others lost significance. These patterns suggest that different RL neurons encode evidence strength at varying thresholds of resolution. Importantly, the observation that some neurons become newly selective at finer difficulty levels echoes findings from Gupta et al. (2024), who showed that internal biases and trial history can shape perceptual choices even when external evidence is ambiguous. It is possible that RL encodes not only sensory inputs, but also belief states updated by experience. This opens an important direction for future work: whether RL represents accumulated sensory evidence, internal states like confidence, or even biases that influence decision thresholds.

To investigate whether particular cell types are preferentially involved in choice encoding, we classified choice-selective neurons by spike waveform into regular-spiking (RS;

typically excitatory) and fast-spiking (FS; typically inhibitory) types (Tremblay et al., 2016). Contrary to initial expectations, the majority of choice-selective neurons were FS (78.9%), with only 4 neurons classified as RS. This suggests a potentially prominent role for inhibitory interneurons in decision-related signaling within RL. The presence of FS neurons in both Left- and Right-choice groups implies that inhibition may help sculpt or gate choice representations through precise temporal modulation. Despite this bias in cell type distribution, we did not observe a strong difference in choice directionality across RS and FS groups, indicating that both cell types contribute to encoding behaviorally relevant signals. These findings add further nuance to our understanding of RL, suggesting that decision-related signals in this region may emerge from coordinated activity between excitatory and inhibitory populations. Combined with the presence of choice-selective neurons, graded difficulty encoding, and dynamic modulation around behavioral responses, these results support the functional definition of RL as a subregion of PPC involved in decision-making. Given RL's connectivity with orbitofrontal cortex and motor-related regions (Gilissen et al., 2021), it may serve as a critical hub linking accumulated evidence with action selection.

Despite these insights, several limitations should be considered. Our analyses focused on firing rate modulations, but did not include more advanced decoding or dimensionality reduction approaches that might reveal latent task variables. While our task minimized impulsive behavior and encouraged evidence accumulation, future work should aim to dissociate sensory input, motor execution, and internal decision states more explicitly. Additionally, causal manipulation, such as inactivation of RL during specific task phases using optogenetics, could clarify whether this region is necessary for choice formation or downstream motor planning.

Nevertheless, this study contributes to growing evidence that RL is not purely a sensory area but instead integrates tactile information to support decision-related processing. By identifying RL neurons that encode trial difficulty and choice direction, we clarify its functional role within the PPC. Although the current findings are limited to animal models, this work may inform future investigations of decision-making circuits and could offer foundational insights for understanding clinical conditions involving deficits in sensory integration and decision-making, such as autism or ADHD (Frost-Karlsson et al., 2024). In this way, our results offer an initial step toward mapping the neural architecture that transforms sensation into choice.

## References

1. Berwick, J., Martin, C., Martindale, J., Jones, M., Johnston, D., Zheng, Y., Redgrave, P., & Mayhew, J. (2002). Hemodynamic response in the unanesthetized rat: intrinsic optical imaging and spectroscopy of the barrel cortex. *Journal of cerebral blood flow and metabolism : official journal of the International Society of Cerebral Blood Flow and Metabolism*, 22(6), 670–679. <https://doi.org/10.1097/00004647-200206000-00005>
2. Brown, E. N., Kass, R. E., & Mitra, P. P. (2004). Multiple neural spike train data analysis: state-of-the-art and future challenges. *Nature neuroscience*, 7(5), 456–461. <https://doi.org/10.1038/nn1228>
3. Brunton, B. W., Botvinick, M. M., & Brody, C. D. (2013). Rats and humans can optimally accumulate evidence for decision-making. *Science (New York, N.Y.)*, 340(6128), 95–98. <https://doi.org/10.1126/science.1233912>.
4. Frost-Karlsson, M., Capusan, A. J., Olausson, H., & Boehme, R. (2024). Altered somatosensory processing in adult attention deficit hyperactivity disorder. *BMC psychiatry*, 24(1), 558. <https://doi.org/10.1186/s12888-024-06002-9>
5. Gallero-Salas, Y., Han, S., Sych, Y., Voigt, F. F., Laurenczy, B., Gilad, A., & Helmchen, F. (2021). Sensory and Behavioral Components of Neocortical Signal Flow in Discrimination Tasks with Short-Term Memory. *Neuron*, 109(1), 135–148.e6. <https://doi.org/10.1016/j.neuron.2020.10.017>
6. Gilissen, S. R. J., Farrow, K., Bonin, V., & Arckens, L. (2021). Reconsidering the Border between the Visual and Posterior Parietal Cortex of Mice. *Cerebral cortex (New York, N.Y. : 1991)*, 31(3), 1675–1692. <https://doi.org/10.1093/cercor/bhaa318>
7. Goard, M. J., Pho, G. N., Woodson, J. & Sur, M. Distinct roles of visual, parietal, and frontal motor cortices in memory-guided sensorimotor decisions. *eLife* 5, e13764 (2016).
8. Gold, J. I., & Shadlen, M. N. (2007). The neural basis of decision making. *Annual review of neuroscience*, 30, 535–574. <https://doi.org/10.1146/annurev.neuro.29.051605.113038>
9. Gupta, D., DePasquale, B., Kopec, C. D., & Brody, C. D. (2024). Trial-history biases in evidence accumulation can give rise to apparent lapses in decision-making. *Nature communications*, 15(1), 662. <https://doi.org/10.1038/s41467-024-44880-5>
10. Han, S., & Helmchen, F. (2024). Behavior-relevant top-down cross-modal predictions in mouse neocortex. *Nature neuroscience*, 27(2), 298–308. <https://doi.org/10.1038/s41593-023-01534-x>
11. Hanks, T. D., Kopec, C. D., Brunton, B. W., Duan, C. A., Erlich, J. C., & Brody, C. D. (2015). Distinct relationships of parietal and prefrontal cortices to evidence accumulation. *Nature*, 520(7546), 220–223. <https://doi.org/10.1038/nature14066>
12. Harvey, C. D., Coen, P., & Tank, D. W. (2012). Choice-specific sequences in parietal cortex during a virtual-navigation decision task. *Nature*, 484(7392), 62–68. <https://doi.org/10.1038/nature10918>
13. Hovde, K., Gianatti, M., Witter, M. P., & Whitlock, J. R. (2019). Architecture and organization of mouse posterior parietal cortex relative to extrastriate areas. *The European journal of neuroscience*, 49(10), 1313–1329. <https://doi.org/10.1111/ejn.14280>
14. Hwang, E. J., Dahlen, J. E., Mukundan, M. & Komiyama, T. History-based action selection bias in posterior parietal cortex. *Nat. Commun.* 8, 1242 (2017).
15. Kass, R. E., Amari, S. I., Arai, K., Brown, E. N., Diekman, C. O., Diesmann, M., Doiron, B., Eden, U. T., Fairhall, A. L., Fiddyment, G. M., Fukai, T., Grün, S., Harrison, M. T., Helias, M., Nakahara, H., Teramae, J. N., Thomas, P. J., Reimers, M., Rodu, J., Rotstein, H. G., ... Kramer, M. A. (2018). Computational Neuroscience: Mathematical and Statistical Perspectives. *Annual review of statistics and its application*, 5, 183–214. <https://doi.org/10.1146/annurev-statistics-041715-033733>
16. Licata, A. M. et al. Posterior Parietal Cortex Guides Visual Decisions in Rats. *J. Neurosci.* 37, 49544966 (2017).
17. Lyamzin, D., & Benucci, A. (2019). The mouse posterior parietal cortex: Anatomy and functions. *Neuroscience research*, 140, 14–22. <https://doi.org/10.1016/j.neures.2018.10.008>

18. Olcese, U., Iurilli, G., & Medini, P. (2013). Cellular and synaptic architecture of multisensory integration in the mouse neocortex. *Neuron*, 79(3), 579–593. <https://doi.org/10.1016/j.neuron.2013.06.010>
19. Pho, G. N., Goard, M. J., Woodson, J., Crawford, B., & Sur, M. (2018). Task-dependent representations of stimulus and choice in mouse parietal cortex. *Nature communications*, 9(1), 2596. <https://doi.org/10.1038/s41467-018-05012-y>
20. Purcell, B. A., Heitz, R. P., Cohen, J. Y., Schall, J. D., Logan, G. D., & Palmeri, T. J. (2010). Neurally constrained modeling of perceptual decision making. *Psychological review*, 117(4), 1113–1143. <https://doi.org/10.1037/a0020311>
21. Raposo, D., Kaufman, M. T., & Churchland, A. K. (2014). A category-free neural population supports evolving demands during decision-making. *Nature neuroscience*, 17(12), 1784–1792. <https://doi.org/10.1038/nn.3865>
22. Ratcliff, R., Hasegawa, Y. T., Hasegawa, R. P., Smith, P. L., & Segraves, M. A. (2007). Dual diffusion model for single-cell recording data from the superior colliculus in a brightness-discrimination task. *Journal of neurophysiology*, 97(2), 1756–1774. <https://doi.org/10.1152/jn.00393.2006>
23. Shadlen, M. N., & Newsome, W. T. (2001). Neural basis of a perceptual decision in the parietal cortex (area LIP) of the rhesus monkey. *Journal of neurophysiology*, 86(4), 1916–1936. <https://doi.org/10.1152/jn.2001.86.4.1916>
24. Sit, K. K., & Goard, M. J. (2020). Distributed and retinotopically asymmetric processing of coherent motion in mouse visual cortex. *Nature communications*, 11(1), 3565. <https://doi.org/10.1038/s41467-020-17283-5>
25. Tremblay, R., Lee, S., & Rudy, B. (2016). GABAergic Interneurons in the Neocortex: From Cellular Properties to Circuits. *Neuron*, 91(2), 260–292. <https://doi.org/10.1016/j.neuron.2016.06.033>
26. Wallis J. D. (2007). Orbitofrontal cortex and its contribution to decision-making. *Annual review of neuroscience*, 30, 31–56. <https://doi.org/10.1146/annurev.neuro.30.051606.094334>
27. Wang, Q., & Burkhalter, A. (2007). Area map of mouse visual cortex. *The Journal of comparative neurology*, 502(3), 339–357. <https://doi.org/10.1002/cne.21286>
28. Weiler, S., Rahmati, V., Isstas, M., Wutke, J., Stark, A. W., Franke, C., Graf, J., Geis, C., Witte, O. W., Hübener, M., Bolz, J., Margrie, T. W., Holthoff, K., & Teichert, M. (2024). A primary sensory cortical interareal feedforward inhibitory circuit for tacto-visual integration. *Nature communications*, 15(1), 3081. <https://doi.org/10.1038/s41467-024-47459-2>
29. Whitlock J. R. (2017). Posterior parietal cortex. *Current biology : CB*, 27(14), R691–R695. <https://doi.org/10.1016/j.cub.2017.06.007>

## Work Plan

Project Description								
My project entails an analysis of electrophysiological neural data collected from the rostralateral (RL) portion of mouse posterior parietal cortex. The electrophysiological data is collected in awake, behaving mice during a two alternative forced-choice task. While some studies have been able to characterize the activity of RL during visual and auditory choice tasks, there is limited data available about the neural activity of RL during tactile evidence accumulation. This project seeks to identify the firing rate and spiking activity of identified neurons in RL and to decode choice-related neurons from these data in order to categorize RL as a part of mouse PPC.								
Tasks/Goals (LMC 4701)	8/25-8/31	9/1-9/7	9/8-9/14	9/15-9/21	9/22-9/28	9/29-10/5	10/6-10/12	
Read and annotate papers sent by mentor (bulleted annotated bib format)	H	H						
Find 5 more papers contextualizing RL/PPC and add to annotated bib		H	L	M	H			
Familiarize with MATLAB code/data from last sem		L	M	H				
MATLAB refresher (online courses, videos, etc)			L	M	H			
Make a list of <i>what</i> questions we want to answer about RL	L		M	H				
List <i>how</i> above questions will be answered (which analyses methods)				L	M	H	L	
Begin analysis (raster) of RL FR from existing data (DW010 and 11)			L	H				
Finish tentative observations of neuron FR and guesses for all experiments						L	H	
	Break Week			Break Week				
Tasks/Goals (LMC 4702)	10/13-10/19	10/20-10/26	10/27-11/2	11/3-11/9	11/10-11/16	11/17-11/23	11/24-11/30	12/1-12/7
Begin training animals on Active				M	M	H	H	
Train animals on Autoreward	M	M	H					
Increase sigma on Active for both animals							L	M
Catch up on incomplete/underdeveloped 'H'	H							
Draft proposal and send to mentor for feedback	L	M	H					
Send proposal to Dr. Stanley + Chris			M	H				
Revise proposal based on feedback				L				
Finalize proposal after receiving feedback					M	H		H
Write introduction of thesis		H						
Test normality and variance	M	H						
Finish stat analysis using Kruskal-Wallis						L	M	H
Tasks/Goals (LMC 4702)	Week 1	Week 2	Week 3	Week 4	Week 5	Week 6	Week 7	
Set big deadlines for submission	H							
Begin writing methods section		L	M	H				
Identify which figures should go in paper			L	M	H			
Finalize figures in MATLAB		L	M	H				
Collect ephys data on another animal	L	L	M	M	M	M	H	
Write figure legends for all figures produced thus far						L	M	
Waveform analysis for excitatory inhibitory			L	M	H			
Have animals training on at least sigma 8				L	M	H		
Spike sorting begin on DW018/9						L	M	
Tasks/Goals (LMC 4702)	Week 8	Week 9	Week 10	Week 11	Week 12	Week 13	Week 14	Week 15
Complete spike sorting data and collection for DW018/9	M	H						
Analyze differences in data with versus without delay (DW010/11 vs 18/19)								
Write conclusions based on results (bullets)	H							
Create rough draft of thesis and send to mentor		L	M	H				
Implement and edit based on feedback from PI + second reader			L	M	H			
Have final draft completed and get approval from PI + second reader					H			
Prepare for thesis presentation					M	H		
Turn in and upload to UROP						L	M	H